

N64 10 977*

The Role of Plasma Instabilities in the Origin of Solar Flares

→ R. K. JAGGI

Theoretical Division, NASA

NASA. Goddard Space Flight Center, Greenbelt, Maryland

CODE ~~DATE~~ ^{DATE} (NASA RP-72)

Abstract. We have investigated the role of plasma instabilities in the origin of a solar flare. Three types of stability problems are discussed: the magnetohydrodynamic instability of an infinitely conducting fluid, the instability due to the magnetic field gradients, and the finite conductivity instability. These instabilities are examined in a situation that occurs when two plasmas trapped in a pair of sunspot magnetic fields approach each other. The assumption of infinite conductivity gives rise to stable situations. The instability growth time in the magnetic field gradients that exist near sunspots is extremely large. The growth time for finite conductivity instability is of the order of a few seconds or minutes, and we therefore believe that the flare can be produced by finite conductivity instabilities in the solar atmosphere above a group of sunspots. Our analysis does not help explain the acceleration of charged particles to high energies; for this, the problem of acceleration must be considered separately.

AUTHOR

1. INTRODUCTION

It has been suggested [Parker, 1962; Dungey, 1961; Gold and Hoyle, 1960] that instabilities may play an important role in explaining the origin of solar flares. Dungey [1961] has suggested that a pinch instability can take place in the ionized solar atmosphere near the neutral point of the sunspot magnetic fields and also that runaway electrons may develop in the transition region, leading to a two-stream instability. The possibility of the pinch instability is based on the assumption that a current may be driven along the neutral point (or line) between two regions of oppositely directed magnetic fields to such an intensity that the self-magnetic field of the current overpowers all other forces. Although this may be a possibility, our analysis in section 2 shows that such an instability does not arise in the equilibria considered here. Gold and Hoyle [1960] consider a particular geometry of a complex sunspot group (in relation to the problem of origin of flares) in which a pair of bipolar sunspots is parallel to another pair of bipolar sunspots. We shall consider here the simpler geometry of four sunspots each of which belongs to a pair of conjugate spots arranged in a straight line. This geometry is considered following Sweet [1958].

Severny [1958, 1959] and Severny and Shab-hanski [1961] have worked out a model of the pinch effect in the neighborhood of the neutral point of the sunspot fields assuming that strong

currents are generated by the magnetic field gradients. Severny arrives at the conclusion that the plasma being compressed by the two sunspot fields is unstable when the magnetic pressure is greater than the kinetic pressure of the plasma. The result is that if a compression begins it will proceed at an ever-increasing rate; i.e., the pinch effect takes place. The phenomena that take place in the chromospheric or coronal plasma near the sunspot region are quite different from the pinch effect produced in the laboratory. Figure 1 shows an equilibrium configuration of the pinched plasma produced in the laboratory. Figure 2 shows one of the possible equilibrium configurations that can arise in the solar plasma before the occurrence of a flare; this case is considered in detail in section 2. The basic difference between the two cases is that, whereas in the first the magnetic field outside the plasma is a decreasing function of the distance, in the second it is uniform. We shall show in section 2 that the equilibrium configuration considered in Figure 2 is stable. The physical reason for the instability of the configuration in Figure 1 is that any plasma moving away from the axis of the cylinder is at a point at which the magnetic field, and therefore the magnetic force, is less, and the perturbation continues to grow. Similarly, if any part of the plasma moves toward the axis of the cylinder it is further pushed by the magnetic field due to the increased magnetic force outside the plasma cylinder. If we now consider the equilibrium

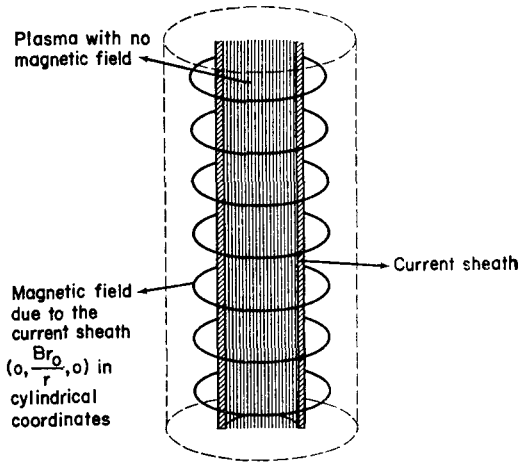


Fig. 1. Pinched plasma produced in the laboratory.

configuration of Figure 2 we at once see that any displacement of the plasma in or out of its region is in the presence of the same magnetic force and there is no cause of instability as in laboratory pinches. The same holds for the equilibrium configuration sketched in Figure 3.

In sections 3 and 4 we shall analyze some of the known instabilities that apply in the present situation, with the understanding that an instability with growth rates of the right order constitutes the flare phenomena, as an insta-

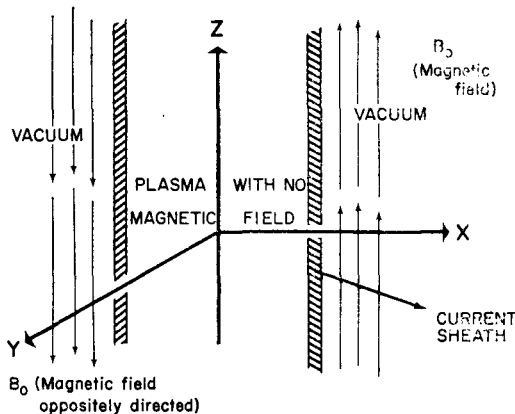


Fig. 2. A possible equilibrium configuration before the onset of flare. The magnetic field on both sides of a zero field region is oppositely directed. Outside is assumed vacuum. The plasma, the current sheath, and the magnetic field extend both ways, perpendicular to the plane of the paper, up to infinity. The current in the sheath flows in the Y direction.

bility helps to blow the material up. The discussion presented here does not help in understanding how the particles get accelerated to energies of the order of a few million electron volts; for this, acceleration processes must be considered separately.

2. MAGNETOHYDRODYNAMIC STABILITY OF EQUILIBRIUM CONFIGURATIONS

Observations show [Saverny, 1958] that, before the occurrence of a flare, the sunspots are approaching each other with the velocity of a few kilometers per second. Assuming that we have a group of four sunspots arranged in a straight line as considered by Sweet [1958, Figure 3], let us suppose that a magnetohydrodynamic equilibrium is reached when the two magnetic fields of the sunspot groups are separated by a distance $2x_0$ with a region of zero magnetic field and hot plasma between. For simplicity, we neglect the gradient of the magnetic field on both sides of the zero field region. The possibility of such an equilibrium configuration will be increased if it is proved that the magnetic field gradients do not give rise to any serious instabilities. In section 3 we will show that the e folding growth time of any perturbation due to the magnetic field gradient instabilities is of the order $10^{0.1}$ seconds. This allows us to neglect any instabilities due to the gradients of the magnetic field. The pressure anisotropy instabilities do not arise in this case

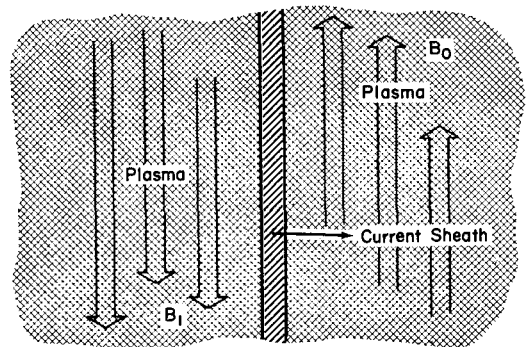


Fig. 3. Another possible hydromagnetic equilibrium of oppositely directed magnetic field regions. The plasma region and the current sheath extended to infinity in Y, Z directions. Right-hand half-plane is filled with plasma with magnetic field $(0, 0, B_0)$ in cartesian coordinates; the left half is filled with plasma with oppositely directed magnetic field $(0, 0, -B_1)$.

CASE FILE COPY

because the collision frequency is sufficiently high in the chromosphere as well as in the corona to preserve the pressure isotropy during the compression of the plasma. For coronal plasma of $N \sim 10^8$ particles/cm³, $T \sim 10^6$ °K, the frequency of electron-electron collisions is of the order of 2.5×10^8 per second and the mean free path of an electron is of the order of 1 km. Since the time involved in the flare process is of the order of minutes, and the length is of the order of thousands of kilometers, the pressure will be assumed isotropic throughout the discussion.

The basic equations in this section are the magnetohydrodynamic equations as used by *Kruskal and Schwarzschild* [1954] and as further employed by *Jaggi* [1962]. With the isotropic pressure the equations of motion are

$$\rho \frac{dv}{dt} + \text{grad } p = \frac{1}{c} \mathbf{j} \times \mathbf{B} \quad (1)$$

$$\frac{\partial \rho}{\partial t} = -\text{div } (\rho \mathbf{v}) \quad (2)$$

$$\frac{\partial \mathbf{B}}{\partial t} = \text{curl } (\mathbf{v} \times \mathbf{B}) \quad (3)$$

$$\frac{1}{p} \frac{dp}{dt} = \frac{\gamma}{\rho} \frac{d\rho}{dt} \quad (4)$$

$$\text{div } \mathbf{B} = 0 \quad (5)$$

$$\text{curl } \mathbf{B} = (4\pi/c) \mathbf{j} \quad (6)$$

where the displacement current has been neglected. As a possible equilibrium configuration for the plasma let us assume that there is no magnetic field in the plasma confined between two parallel planes $x = \pm x_0$. For $x > x_0$ there is vacuum and the magnetic field $(0, 0, B_0)$ is constant and parallel to the surface. Taking the z axis parallel to this magnetic field, we have a current in the y direction at $x = \pm x_0$. For $x < x_0$ the magnetic field is $(0, 0, -B_0)$. The boundary conditions are

$$\mathbf{n} \cdot [\mathbf{B}] = 0 \quad (7)$$

$$[p + (B^2/8\pi)] = 0 \quad (8)$$

If we perturb the boundary of the plasma-vacuum interface as

$$x = \pm x_0 + i \frac{(v_n)x = \pm x_0}{\omega} e^{ik_2 y + ik_3 z - i\omega t} \quad (9)$$

where the perturbations of the physical entities in the plasma are of the form (e.g., the perturbation in the pressure denoted by subscript 1)

$$p_1 = p_1(x) e^{ik_2 y + ik_3 z - i\omega t} \quad (10)$$

Linearizing equation 4 gives

$$p_1 = \zeta^2 \rho_1 \quad (11)$$

where $\zeta = \sqrt{\gamma p_0/\rho_0}$ is the velocity of sound in the plasma, and p_0 and ρ_0 are the equilibrium pressure and density of the plasma, respectively. We easily find that

$$\mathbf{B}_1 = 0 \quad (12)$$

ρ_1 satisfies the equation

$$\frac{\partial^2 \rho_1}{\partial x^2} - (k_1^2 + k_2^2 - \omega^2/\zeta^2) \rho_1 = 0 \quad (13)$$

and has for its solution

$$\rho_1 = A e^{Kx} + B e^{-Kx} \quad (14)$$

with $K = \sqrt{k_1^2 + k_2^2 (\omega^2/\zeta^2)}$.

Also

$$p_1 = \zeta^2 (A e^{Kx} + B e^{-Kx}) \quad (15)$$

$$\left. \begin{aligned} v_x &= -\frac{i\zeta^2 k}{\omega \rho_0} (A e^{Kx} - B e^{-Kx}) \\ v_y &= \frac{\zeta^2 k_2}{\omega \rho_0} (A e^{Kx} + B e^{-Kx}) \\ v_z &= \frac{\zeta^2 k_3}{\omega \rho_0} (A e^{Kx} + B e^{-Kx}) \end{aligned} \right\} \quad (16)$$

The solutions for perturbation in magnetic field in the vacuum $x > x_0$ and $x < x_0$ are, respectively,

$$\left. \begin{aligned} B_{1x} &= D K_1 e^{-K_1 x} \\ B_{1y} &= D i k_2 e^{-K_1 x} \\ B_{1z} &= D i k_3 e^{-K_1 x} \\ B_{1x} &= D_1 K_1 e^{K_1 x} \\ B_{1y} &= D_1 i k_2 e^{K_1 x} \\ B_{1z} &= D_1 i k_3 e^{K_1 x} \end{aligned} \right\} \quad (17-18)$$

and

where $K_1 = \sqrt{k_2^2 + k_3^2}$ and D and D_1 are constants of integration; the factor $e^{ik_2 y + ik_3 z - i\omega t}$ has been omitted on both sides of equations 14

and 17-18 for convenience. Applying the boundary conditions (7) and (8) at $x = +x_0$ and $x = -x_0$, we obtain the dispersion equations

$$\left. \begin{aligned} \omega^2 \frac{K_1}{V_A^2 k_3^2 k} (e^{2Kx_0} - 1) &= (e^{2Kx_0} + 1) \\ \text{or} \\ \omega^2 \frac{K_1}{V_A^2 k_3^2 k} (e^{2Kx_0} + 1) &= (e^{2Kx_0} - 1) \end{aligned} \right\} \quad (19)$$

which show that ω^2 cannot be negative, and therefore the equilibrium is stable.

The other equilibrium configuration considered by us is shown in Figure 3. For $x > 0$, we have a uniform plasma of density ρ_0 , pressure p_0 , and the magnetic field $(0, 0, B_0)$. For $x < 0$, we have a uniform plasma of density ρ_1 , pressure p_1 , and magnetic field $(0, 0, -B_1)$. At $x = 0$, we have a current $(c/4\pi)(B_1 - B_0)$ in the y direction. Following the analysis given above, we obtain the dispersion equation in the form

$$\left[k_2^2 + k_3^2 + \frac{\left(1 - \frac{\omega^2}{k_3^2 c_0^2}\right) \left(1 - \frac{\omega^2}{k_3^2 V_0^2}\right)}{\left(1 - \frac{\omega^2}{k_3^2 c_0^2} - \frac{\omega^2}{k_3^2 V_0^2}\right)} \right]^{1/2} \cdot \left[k_2^2 + k_3^2 + \frac{\left(1 - \frac{\omega^2}{k_3^2 c_0^2}\right) \left(1 - \frac{\omega^2}{k_3^2 V_0^2}\right)}{1 - \frac{\omega^2}{c^2 k_3^2} - \frac{\omega^2}{k_3^2 V_1^2}} \right]^{1/2} = - \frac{\left(1 - \frac{\omega^2}{k_3^2 V_0^2}\right)}{\left(1 - \frac{\omega^2}{k_3^2 V_1^2}\right)} \quad (20)$$

where

$$\begin{aligned} c_0 &= \sqrt{\gamma p_0 / \rho_0} & c_1 &= \sqrt{\gamma p_1 / \rho_1} \\ V_0 &= B_0 / \sqrt{4\pi \rho_0} & V_1 &= B_1 / \sqrt{4\pi \rho_1} \end{aligned}$$

If $\omega^2 < 0$, the left-hand side is positive and the right-hand side negative. This shows that no solution is possible for $\omega^2 < 0$; i.e., no instabilities exist. For $B_0 = B_1$, $\rho_0 = \rho_1$, $p_0 = p_1$, i.e., the symmetrical case, the dispersion equation is of the form

$$k_2^2 + k_3^2 \frac{\left(1 - \frac{\omega^2}{k_3^2 c_0^2}\right) \left(1 - \frac{\omega^2}{k_3^2 V_0^2}\right)}{\left(1 - \frac{\omega^2}{k_3^2 c_0^2} - \frac{\omega^2}{k_3^2 V_0^2}\right)} = 0 \quad (21)$$

which gives a quadratic equation having two positive roots. Thus there are no instabilities of the current layer in equilibrium between two ionized clouds having oppositely directed uniform magnetic fields. If we take the gradient of the magnetic field into account we predict that the current layer will still be stable because the magnetic field on both sides has increasing magnitude.

3. MAGNETIC FIELD GRADIENT INSTABILITIES

We shall now show that there are no serious magnetic field gradient instabilities for long wavelengths to affect the assumption of the equilibrium configurations studied in the previous section. Krall and Rosenbluth [1962] have considered a plasma in equilibrium in a magnetic field of the form

$$B = B_0(1 + \epsilon x)i_z \quad (22)$$

where i_z is a unit vector in the z direction. This magnetic field configuration is quite suitable for our problem. The distribution function for the electrons and ions can be assumed to be

$$f_{0i} = n \left(\frac{\alpha_i}{\pi^2} \right) \left(\frac{\beta_i}{\pi} \right)^{1/2} \exp[-\alpha_i(v_z^2 + v_y^2)] \cdot \exp[-\beta_i(v_z^2)] g \quad (23)$$

where the subscript j refers to electrons ($j = e$) and ions ($j = i$); g satisfies the equation

$$\frac{dg}{dx} - \frac{eB_0}{mc} [1 + \epsilon x] \frac{dg}{dy} = 0 \quad (24)$$

Choosing

$$\begin{aligned} g_e &= 1 - \epsilon^2 \left(x + \frac{1}{2} \epsilon x^2 - \frac{vy}{\Omega_e} \right) \\ g_i &= 1 - \epsilon^2 \left(n + \frac{1}{2} \epsilon x^2 + \frac{vy}{\Omega_i} \right) \end{aligned}$$

where $\epsilon^2 = eB_0^2/[4\pi n k(T_e + T_i)]$, n being the number density of the particles, $\Omega_e = eB_0/mc$, $\Omega_i = eB_0/Mc$, m = the mass of the electron and M that of an ion, Krall and Rosenbluth arrive at unstable solutions of the form e^{st} with the growth rate s given by

$$\begin{aligned} R_e(s) &= 2 \left(\frac{T_e}{T_i} \right)^2 \frac{\pi \Omega_i}{X k^2 R_i^2} E_i \left(X \frac{T_i}{T_e} \right) \exp \left(\frac{2XT_i}{T_e} \right) \\ &\quad \{ [E_i(XT_i/T_e)]^2 + \pi^2 \}^2 \end{aligned} \quad (25)$$

for $k R_e < 1$, $\epsilon_1/\epsilon \gg 1$, and

$$R_e(s) = \frac{4\Omega_i \left(\frac{T_e}{T_i}\right)^{3/2} \exp\left(\frac{2XT_i}{T_e}\right) {}_1F_1\left(\frac{1}{2}, \frac{3}{2}; \frac{XT_i}{T_e}\right)}{X(\pi X)^{1/2} \left\{ \frac{4T_i}{\pi T_e} \left[{}_1F_1\left(\frac{1}{2}, \frac{3}{2}; \frac{XT_i}{T_e}\right) \right]^2 + \frac{1}{X} \right\}^2} \quad (26)$$

for $k R_e > 1$, $\epsilon_1/\epsilon \gg 1$, where R_e and R_i denote the Larmor radii of electrons and ions respectively. Here $X = 2d_i\Omega_i^2/k_e$ should not be confused with the coordinate x . k is the wave number of purely longitudinal electrostatic oscillations of the form

$$\mathbf{E} = (E\mathbf{k}/|k|)\epsilon^{ik\cdot\mathbf{r}}E_i(XT_i/T_e) \\ \simeq e^{X T_i/T_e}/(XT_i/T_e)$$

for large values of X , and ${}_1F_1$ is a confluent hypergeometric function. For the case of sunspot magnetic field gradients,

$$\epsilon = \frac{1}{B} \frac{dB}{dx} \simeq \frac{1}{10^{10}} \text{ cm}^{-1}$$

$$B_0 \sim 10^3 \text{ gauss}$$

$$X \simeq 0.243(B^2\lambda/T_i)$$

where $\lambda = 2\pi/k$. For $T = 5 \times 10^3$ °K, $\lambda \simeq 1$ cm, $X \simeq 10^{13}$, i.e., an extremely large quantity. Equation 25 yields

$$R_e(s) \simeq \frac{10_1^{21}}{6} \frac{10^{36}}{e^{10^{13}}} \sim 10^{-10^{13}} \quad (27)$$

i.e., an extremely small number.

Conversely, if $k R_e > 1$, i.e., wavelengths less than the electron cyclotron radius, the growth rate is extremely large, of the order of inverse of the growth rate for $k R_e < 1$. This shows that only extremely small wavelengths are unstable. The Debye length in the lower chromosphere is $(kT/4\pi ne^2)^{1/2} \simeq 5 \times 10^{-2}$ cm, and the electron cyclotron radius corresponding to 5×10^3 °K temperature is of the order of 10^{-3} cm. Any wavelengths less than the electron cyclotron radius will also be less than the Debye length, and the theory may not apply. (This is satisfied in the corona as well.) At any rate, the instability of extremely small wavelength, although taking place instantaneously, will not be efficient to enhance the thermal and electrical diffusion of the plasma.

The magnetic field gradient instabilities discussed so far in this section are only important much before the equilibrium between the magnetic pressure and the kinetic pressure is reached (if it is reached at all) because of the condition $\epsilon_1/\epsilon \gg 1$ imposed on solutions 25 and 26. After the compression continues, the temperature of the plasma builds up; the pressure P begins to increase until it is comparable with the magnetic pressure $B^2/8\pi$. The kinetic pressure develops more rapidly than the magnetic field pressure [Severny, 1958, p. 321], and an equilibrium configuration can be reached when P is comparable with $B^2/8\pi$.

It might be thought that the pressure anisotropy instabilities can develop in this case, but it can be shown that owing to the slow rate of approach of the two sunspots and owing to the high collision frequency the pressure anisotropy cannot develop to the extent of producing an instability. As has been mentioned earlier, the collision frequency in the lower corona is of the order of about 10^8 per second, and, since the compression time is of the order of hundreds of seconds, the collisions will keep the pressure quite isotropic in the present situation. It is only if the phenomena take place in about 10^{-4} second that the pressure anisotropy can be important. To calculate the magnetic field, the density, and the temperature after the compression we may use the adiabatic equations deduced by Chew, Goldberger, and Low [1956]. With $P_{\parallel} = P_{\perp}$, these equations are

$$\frac{PB^2}{N^3} = \text{constant} \quad (28)$$

$$\frac{P}{NB} = \text{constant} \quad (29)$$

from which we obtain

$$\frac{B^3}{N^2} = \text{constant} \quad (30)$$

If L_0 , B_0 , P_0 denote the initial length, magnetic field density, and the pressure of the plasma, the quantities B_1 , N_1 , P_1 for a given L_1 can be calculated from $N_1 L_1 = N_0 L_0$, $B_1^3/N_1^2 = B_0^3/N_0^2$, $P_1/N_1^{5/3} = P_0/N_0^{5/3}$. For $B_0 = 10^3$ gauss, $N_0 = 10^{12}/\text{cm}^3$, $L_0 = 10^{10}$ cm, $T_0 = 5 \times 10^3$ °K, we obtain for $L_1 = 10^7$ cm, $N_1 = 10^{15}/\text{cm}^3$, $B_1 = 10^5$ gauss, $T_1 = 5 \times 10^6$ °K. The collision

frequency remains about the same as before the compression.

4. RESISTIVE INSTABILITIES

The instabilities discussed so far apply in the case of infinite conductivity of the plasma under consideration. Recently some work has been done assuming finite conductivity of the plasma [Furth *et al.*, 1963]. We shall use the results to make an estimate of the growth rates of resistive instabilities.

The infinitely thin current layer as sketched in Figure 3 will now be assumed to have finite thickness denoted by a . We will also assume a magnetic field in the current layer. With finite conductivity, equation 3 has to be replaced by

$$\frac{\partial \mathbf{B}}{\partial t} = \text{curl}(\mathbf{v} \times \mathbf{B}) - \text{curl} \left[\frac{\eta}{4\pi} \text{curl} \mathbf{B} \right] \quad (31)$$

where η is the isotropic resistivity of the plasma. The magnetic field in the current sheath has the form

$$\mathbf{B} = i_z B_z(x) \quad (32)$$

Further assuming the current layer to be incompressible (this amounts to using $\text{div} \mathbf{v} = 0$ in place of equation 2 and deleting equation 4), two unstable modes are deduced by Furth, Killeen, and Rosenbluth for waves propagating in the z direction. They are called the rippling mode and the tearing mode. The rippling mode arises in the case in which the resistivity varies with distance in the current layer; the growth rate of the instability which is the inverse of the e folding time of a perturbation is given by

$$R_* (s) = \alpha^{2/5} S^{2/5} / 4\pi a^2 \sigma \quad (33)$$

where $\sigma (=1/\eta)$ is the conductivity of the plasma in emu

$$S = 10^{-2} \frac{T^2}{\sqrt{4\pi P_0/B_0}}$$

T in electron volts, $\alpha = ka$, where k is the wave number of waves in the current layer (propagating in the current layer). Also this instability occurs for $S^{-2/7} < \alpha < S^{2/3}$. Using $\sigma = 2 \times 10^{-14} T^{3/2}$ emu, $T = 10^6$ °K, $a = 10^6$ cm (10^6 °K \cong 86 ev), we have $S = 7 \times 10^3$, and the e folding time which is the inverse of R_* (s) is of the order of $10^3/k^{2/3}$. Now, from $S^{-2/7} < \alpha < S^{2/3}$ we get $2.8 < 1/k < 10^6$. For long wavelengths, the e folding time for the rippling mode is large. Only for small wavelengths, of the order of a few centimeters, the times are reasonable and the instability of rippling mode is important for the problem in hand.

The tearing mode is unstable for $\alpha < 1$ or wavelengths greater than the thickness of the current sheath. In this case the e folding time is of the order $10^6 k^{2/5}$, where $k \lesssim 1/2500$. This time will be small for long wavelengths, and the order of magnitude is also suitable for the problem.

The above results are derived on the assumption that the current layer is incompressible, and it is proved by Furth, Killeen, and Rosenbluth that the results are not much different if compressibility is taken into account.

To arrive at the above figures, we have used the temperature of 10^6 °K in the higher chromospheric region. Some people [De Jager, 1959, 1961] are of the opinion that the temperature of the chromosphere region does not rise very much and that only the density becomes higher. A differing view, based on theoretical models, is adopted in section 3 of this article, following Severny [1958]. For this reason we have evaluated the growth rates of rippling and tearing modes in Table 1. The magnetic field at the neutral point, where the current sheath is formed, will be weak. This is another reason why the growth rate can drop off by several orders of magnitude.

TABLE 1. Rippling and Tearing Mode Instability

If t_r denotes the e folding time for the rippling mode, this table evaluates $t_r(k)^{2/5} = 2.96 \times 10^{-2} T^{9/10}/B_0^{2/5}$. The e folding time for the tearing mode is obtained from $t_t = t_r 10^4(k)^{1/5}$.

T , °K	$B = 10$ gauss	$B = 10^2$ gauss	$B = 10^3$ gauss	$B = 10^4$ gauss	$B = 10^5$ gauss	$B = 10^6$ gauss
10^4	44.4	18.6	7.42	2.96	1.17	0.469
10^5	3.7×10^2	1.48×10^2	59	23.5	9.35	3.72
10^6	2.96×10^3	1.17×10^3	4.69×10^2	1.78×10^2	74.03	29.6
10^7	3.72×10^3	1.47×10^3	5.9×10^2	2.24×10^2	93.02	36.58

For the rippling mode the e folding time is obtained by multiplying each member of the table by $(k^{-1})^{2/5}$. We find that $\frac{6.7}{30.7} > (k^{-1})^{2/5} > \frac{1}{10^{-3}}$ for the whole range of the table. The upper numbers apply for $B = 10$, $T = 10^4$; the lower, for $B = 10^6$, $T = 10^7$. An intermediate value of 1 shows that suitable time scales are obtained for almost all the values of B and T in the table. The above results are deduced for $N \sim 10^{15}$ particles/cm³. If, instead, we use $N \sim 10^{12}$ particles/cm³, it amounts to multiplying each number in the table by $10^{3/5} \sim 4$. N occurs in t_r or t_i as $N^{-1/5}$.

For the tearing mode the e folding time is obtained by multiplying each member of the table by $10^4(k)^{2/5}$, where, for the whole range of the table, $10^{-2} > (k)^{2/5} > 0.0208$. The upper number applies for $B = 10$, $T = 10^4$; the lower, for $B = 10^6$, $T = 10^7$. Assuming $k^{2/5}$ to be of the order of 10^{-3} , we see that the e folding times, for large magnetic fields and small temperatures, are reasonable. We therefore conclude that the resistive instabilities give reasonable times for the problem in hand.

Acknowledgments. I should like to thank Drs. J. M. Burgers, W. N. Hess, E. N. Parker, and D. A. Tidman for stimulating discussion.

I was a NAS Research Associate during this work.

REFERENCES

- Chew, G. F., M. L. Goldberger, and F. E. Low, An attempted derivation of a one-fluid magnetohydrodynamics, *Proc. Roy. Soc. London, A*, **236**, 112, 1956.
- De Jager, C., Structure and dynamics of the solar atmosphere, *Handbuch der Phys.*, **52**, 80, Springer, Göttingen, 1959.
- De Jager, C., The development of a solar center of activity, *Vistas in Astronomy*, edited by A. Beer, vol. 4, pp. 143-183, Pergamon Press, 1961.
- Dungey, J. W., *Kyoto Conf. Cosmic Rays and Earth Storms (IAU)*, Kyoto, Japan, 1961.
- Furth, H., J. Killeen, and M. N. Rosenbluth, Finite resistive instabilities of a sheet pinch, to be published in *Phys. Fluids*, 1963.
- Jaggi, R. K., Magnetohydrodynamic stability of a self-gravitating plasma, *Z. Astrophys.*, **54**, 190, 1962.
- Gold, T., and F. Hoyle, On the origin of solar flare, *Monthly Notices Roy. Astron. Soc.*, **122**, 89-105, 1960.
- Krall, N., and M. N. Rosenbluth, Trapping instabilities in a slightly inhomogeneous plasma, *Phys. Fluids*, **5**, 1435, 1962.
- Kruskal, M., and M. Schwarzschild, Some instabilities of a completely ionized plasma, *Proc. Roy. Soc. London, A*, **223**, 348, 1954.
- Parker, E. N., Theory of reconnection and annihilation of magnetic fields with application to solar flares and interstellar space, unpublished, 1962.
- Severny, A. B., Nonstationary processes in solar flares as a manifestation of the pinch effect, *Soviet Astron. (A.J.)*, **2**, 310, 1958.
- Severny, A. B., On the appearance of cosmic rays in the pinch effect in solar flares, *Soviet Astron. (A.J.)*, **3**, 223, 1959.
- Severny, A. B., and V. P. Shabanskii, The generation of cosmic rays in flares, *Soviet Astron. (A.J.)*, **4**, 583, 1961.
- Sweet, P. A., The neutral point theory of solar flares, *IAU Symp. on Electromagnetic Phenomena in Cosmical Phys.*, **6**, 123, 1958.

(Manuscript received March 30, 1963.)